J Mater Sci (2006) 41:5751–5757
DOI 10.1007/s10853-006-0106-8

LETTER

Si_3N_4/Mg composites with an interpenetrating network

Wang Shou-ren · Geng Hao-ran · Wang Ying-zi

Received: 29 May 2005 / Accepted: 6 December 2005 / Published online: 8 June 2006
© Springer Science+Business Media, LLC 2006

Introduction

Metal matrix composites (MMCs) have some kinds of reinforcement such as particle , whisker and fibre [1–3] as well as three dimensional network structure (3DNMMCs) [4]. In recent years, the MMCs reinforced by 3DNMMCs have been received much attention [5]. Especially, 3DNMMCs reinforced by ceramic phase with an interconnected interpenetrating network structure have become of great interest because of their attractive microstructure and properties [6, 7]. For example, the Si_3N_4 ceramic with network structure interpenetrating ductile metal magnesium would take an amazing effects in microstructure and properties due to the ceramic phase providing low density, high elastic modulus and high strength while the metallic phase offering high toughness as well as high thermal and electrical conductivity [8, 9]. Such composites can be produced by infiltration of a molten metal into porous ceramic skeleton under or without pressure. Porous ceramic skeleton can be fabricated by a variety of methods such as replication technique, gas bubble formation and space holder methods [10, 11]. The most common method of making an open cell ceramic foam skeleton is replication technique, which has been known for almost 40 years (which was first developed in the early 1960s) [12]. Polymer foam of desired high open pore is immersed into a low viscosity ceramic slurry, thereby burn out and finally sintered [10, 13]. The infiltration technique is the most attractive processing route to fabricate 3DNRMMCs which can be classified into three categories based on the source of driving force: pressure assisted, vacuum driven and pressureless or capillarity driven [14]. These methods cause a great contact area between the components [14]. During this process the interfacial reactions between metal and ceramic can take place, which leads to the appearance of a spinel phase on the ceramic/metal interface. The interface characteristic decides about the properties of the composites.

In this paper, the authors attempt to attribute the microstructure of porous ceramic skeleton and increase investigations of the ceramic/metal interface where products of a reaction between the liquid metal and the ceramics can appear. Preliminary results of studies of Si_3N_4/Mg composites obtained via infiltration of a porous Si_3N_4 ceramic skeleton are reported.

W. Shou-ren (✉)
The Key Laboratory of Liquid Structure and Heredity of Materials of Shandong University, Jiwei Road 106#, Jinan 250014, China
e-mail: sherman0158@tom.com

W. Shou-ren
School of Mechanical Engineering, Jinan University, Jinan 250022, China

G. Hao-ran · W. Ying-zi
School of Material Science, Jinan University, Jinan 250022, China

Experimental procedure

Fabrication of porous ceramic skeleton

A commercial β-Si_3N_4 powder ($Si_3N_4 \geq 97\%$, diameter ≤ 100 μm, supplied by Shanghai Silicon Materials Plant, China) was used as starting material to fabricate the porous ceramic skeleton. The sintering additives as 5 wt%ZrO_2 and 2 wt%Al_2O_3 ($Al_2O_3 \geq 99.66\%$, diameter ≤ 90μm, supplied by Shandong Aluminum Industry Company, China) and 5 wt%Al (Al ≥ 99.26%, $D_{50} = 4 \pm 1.5$ μm, supplied by

Shandong Aluminum Industry Company, China) were mixed with the starting materials and ball-milled for 4 h using Al_2O_3 balls. A commercial silica sol (SiO_2, 30.0–31.0%; pH, 8.5–10.0, supplied by Shanghai Kangning Silica Sol Company, China) was used as a binder to be added in the resulting powder mixture. A kind of surfactant carboxymethyl cellulose was added to serve as a wetting agent. The commercial polyurethane sponges (PUS, supplied by Shanghai Nanjia Sponges Production Company, China) with reticulated structure, interconnected struts and open porosity of approximately 10 pores per inch (ppi) were chosen in this study. The cleared PUS was cut into standard form of ϕ 30 × 100 mm and immersed into the homogeneous slurry for about 10 min. The samples were placed into the drying oven under 160 °C for at least 20 h. The sintering process was carried through at 1400 °C for 2 h in oxidizing atmosphere and followed by cooling in the furnace to room temperature. The representative images of the macroscopic structure of porous reticulated ceramic were presented in Fig. 1. All these samples were selected as a potential ceramic phase to the experiments of infiltration by magnesium metal.

Fabrication of Si_3N_4/Mg composites

The chemical compositions for the alloy (which was shown in Table 1) for the infiltration were prepared in a resistance furnace under a protective atmosphere of N_2 (99.996%) to avoid oxidation. Pure Al (99.99%), Mg (99.96%), and Mg-3%Bi alloy were used as raw materials to prepare the alloys. The preforms were heated in N_2 at a rate of 15 °C/min up to the test temperature. After achieving the infiltration temperature, the liquid metal magnesium was infiltrated into the preform skeleton based on capillarity driven. Two specimens (*B* and *C*) at different process parameters as infiltration temperature (*T*), infiltration time (t_I) and heat hold time (t_H) were fabricated. Those different processes lead to different interface characteristics and properties such as compressive strength (σ_C), prolongation (*L*) and tensile strength (σ_T) (as shown in Table 2, specimen *A* as the alloy). The micro-structural characteristic of Si_3N_4/Mg composites with a three-dimensional interpenetrating network was performed on a scanning electron microscopy (SEM, HITACHI, Model No. S-2500) which presented in Fig. 2.

Table 1 The chemical compositions for magnesium alloy, wt%

Mg	Bi	Zn	Al	Si	Ti	Ni	Cu
90.328	0.108	1.132	8.33	0.04	0.043	0.014	0.005

Table 2 The infiltration processes and properties of alloy and 3DNMMCs

Specimen	T (°C)	t_I (min)	t_H (min)	σ_C (MPa)	L (%)	σ_T (MPa)
A	–	–	–	240	5	230
B	1050	150	180	250	2	241
C	920	60	60	255	2	49

Results and discussion

Microstructure of the porous ceramic skeleton

The relative density of porous ceramic was measured by using the Archimedes' method. The pore size was determined by the bubble method [15]. In this method the pore size is defined by the pressure required for the first air bubble to be pressed out by the porous sample. The width of strut (t), the length of strut (l) (which was shown in Fig. 3) and the number of pore were also determined by the microstructure of porous ceramic skeleton such as Fig. 4. In order to obtain relatively accurate results, the method of statistical treatment is necessary to be used. The cross-section and surface micro-structural characterization of the samples were performed on a SEM (HITACHI, Model No. S-2500). The obtained results are presented in Table 3. The relative density was validated by the following equation [16]:

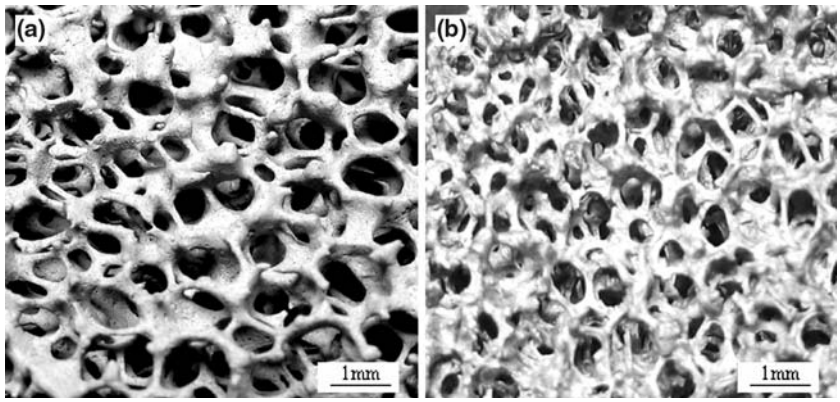

Fig. 1 Porous reticulated ceramic structure. (**a**) Before sintering (**b**) after sintering at 1400 °C

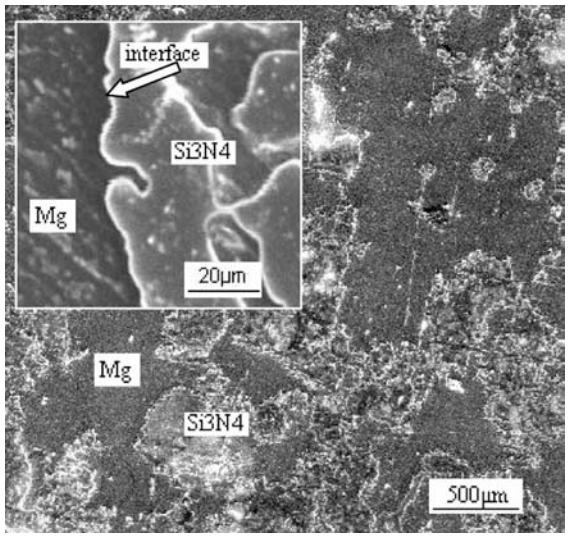

Fig. 2 The microstructure of Si_3N_4/Mg composites with an interpenetrating network. The bright phase is Si_3N_4 ceramic skeleton, the dark phase is magnesium

Table 3 The parameters of porous ceramic skeleton

The number of pore (ppi)	Pore size (d, mm)	Struts width (t, mm)	Struts length (l, mm)
10 ± 2	3 ± 0.5	2.7 ± 0.5	7 ± 1

$$\frac{\rho^*}{\rho_s} = C\left(\frac{t}{l}\right)^2\left[1 - D\left(\frac{t}{l}\right)\right] \qquad (I)$$

where ρ^* is the density of porous solid, ρ_s is the density of the fully dense solid material, C, D is the constant, $C = 1.2$, $D = 0.7$ [17]. The density and porosity of porous ceramic skeleton are shown in Table 4.

The sintering additives as Al powder would be melted gradually with the increasing sintering temperature above 700 °C during the fabrication process of porous ceramic. The liquid Al at elevated temperature was diffused in the solid phases, thereby removing the cracks and jamming the hollow struts in the ceramic foam (as shown in Fig. 3). The additives of Al_2O_3 and ZrO_2 and in situ SiO_2 produced a glass phase at a higher temperature above 1300 °C. Owing to the existing of the additives, there should be few cracks in the struts, and the central void itself would lose the sharp

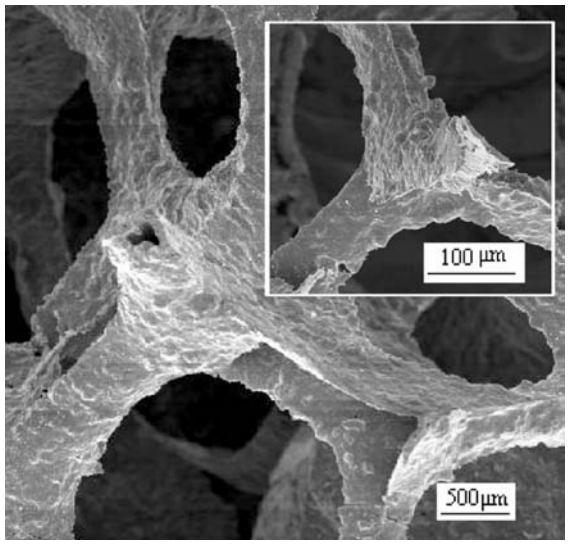

Fig. 4 Microstructure of Si_3N_4 porous ceramic skeleton (SEM)

Table 4 The density and porosity of porous ceramic skeleton

Density of porous solid (g/cm^3)	Density of solid material (g/cm^3)	Relative density (g/cm^3)	Calculation result (g/cm^3)	Open porosity (%)
0.581 ± 0.05	3.17 ± 0.05	0.186 ± 0.02	0.185	81.4 ± 2

edged features typical of other reticulated foams as shown in Fig. 5a. Central void has a round appearance as shown in Fig. 5b and the hollow struts were jammed as shown in Fig. 5c.

Si_3N_4/Mg composites ceramic/metal interface

It is a well known fact that interfacial reactions take place in most of the ceramic–metal systems. For example, In the composite Al_2O_3–Fe, The iron aluminate spinel formation takes place at temperatures above 1000 °C [5]. In Al_2O_3/Al–Mg composites, Mg reacts with alumina, and $MgAl_2O_4$ spinel forms at the ceramic/metal interface [18]. A similar situation is observed between Mg and Si_3N_4. It can take place during the process of pressureless infiltration of melted magnesium into the porous Si_3N_4 ceramic network structure. In Si_3N_4/Mg

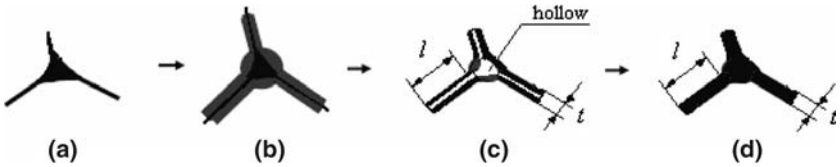

Fig. 3 The fabrication process and the struts parameters of porous ceramic. (**a**) Polymer strut, (**b**) polymer strut coated with ceramic slurry, (**c**) ceramic skeleton with hollow struts, (**d**) ceramic skeleton with jammed struts.

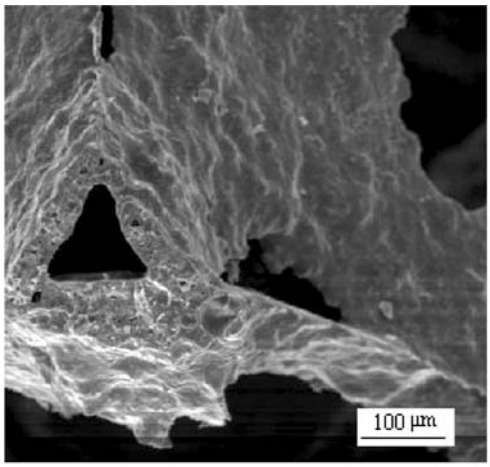

(a) The hollow struts with a sharp edged features

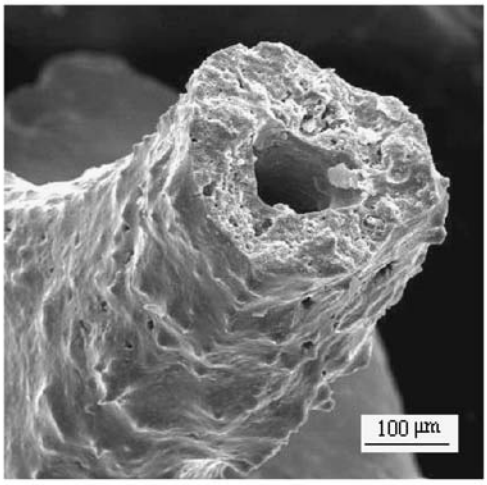

(b) The hollow struts with a round appearance

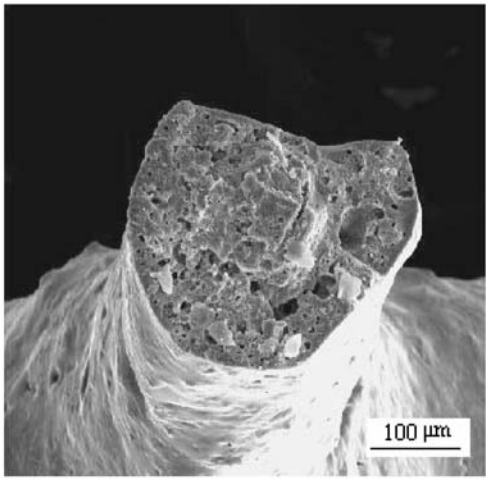

(c) The jammed struts of porous ceramic

Fig. 5 Microstructure of struts of Si_3N_4 porous ceramic skeleton. (**a**) The hollow struts with a sharp edged features, (**b**) the hollow struts with a round appearance, (**c**) the jammed struts of porous ceramic

composites, the strut surface of Si_3N_4 ceramic formed a oxide film of Al_2O_3 and SiO_2 (Fig. 6a) due to the ceramic materials sintered at oxidizing atmosphere, as was shown by the energy spectrum analyses (ESA, OXFOED INCA) in Fig. 6b. The result was confirmed by XRD analyses as shown in Fig. 7. In this experiment, the sintered ceramic powder was attained by crushing the porous ceramic skeleton.

It was indicated that the ceramic/metal interface contained rich Mg, Al, Si and O, which formed interfacial reaction product $MgAl_2O_4$ spinel. The interface reactions are shown as follow:

$$4Al_2O_3 + 3Mg \rightarrow 3MgAl_2O_4 + 2Al$$
$$\Delta G^{\circ} = -201.8 \text{ kJ mol}^{-1}, \quad \Delta H^{\circ} = -194.2 \text{ kJ mol}^{-1} \qquad (1)$$

$$Mg + 2Al + 2SiO_2 = MgAl_2O4 + 2Si$$
$$\Delta G^{\circ} = -464.2 \text{ kJ mol}^{-1}, \quad \Delta H^{\circ} = -479 \text{ kJ mol}^{-1} \qquad (2)$$

$$2Mg + SiO_2 = 2MgO + Si$$
$$\Delta G^{\circ} = -282.2 \text{ kJ mol}^{-1}, \quad \Delta H^{\circ} = -293.2 \text{ kJ mol}^{-1} \qquad (3)$$

$$2MgO + 4Al + 3SiO_2 = 2MgAl_2O_4 + 3Si$$
$$\Delta G^{\circ} = -646.2 \text{ kJ mol}^{-1}, \Delta H^{\circ} = -664.8 \text{ kJ mol}^{-1} \qquad (4)$$

On the one hand, the above reactions (1)–(4) are expected to take place($\Delta G < 0$) since $MgAl_2O_4$ is a thermodynamically stable phase in the Al–Mg–O system. The paper [19] confirmed that when Mg composition is above 0.1 wt%, the reactions would occur spontaneously. The Mg content used in this study is much more rich and the reaction terminated when the count of Al_2O_3 and SiO_2 deplete entirely. The growth of spinel layer is controlled by the counter diffusion of Mg^{2+} ions [18]. On the other hand, reactions (1)–(4) are exothermal reaction ($\Delta H < 0$), the heat quantity decreases turn slowly in infiltration front and this redound to pressureless infiltration. On the ceramic/metal interface a layer of the spinel phase is visible (Fig. 8). The thickness of the spinel layer was between 500 and 6000 nm, literature [14] has got the similar conclusion.

The spinel phase at the ceramic/metal interface plays a significant role in determining the mechanical properties of 3DNMMCs, such as compressive strength, tensile strength and wear resistance. This attributes to the thickness and morphology of the spinel. Above viewpoint has already been discussed in the literature. Some authors report that a

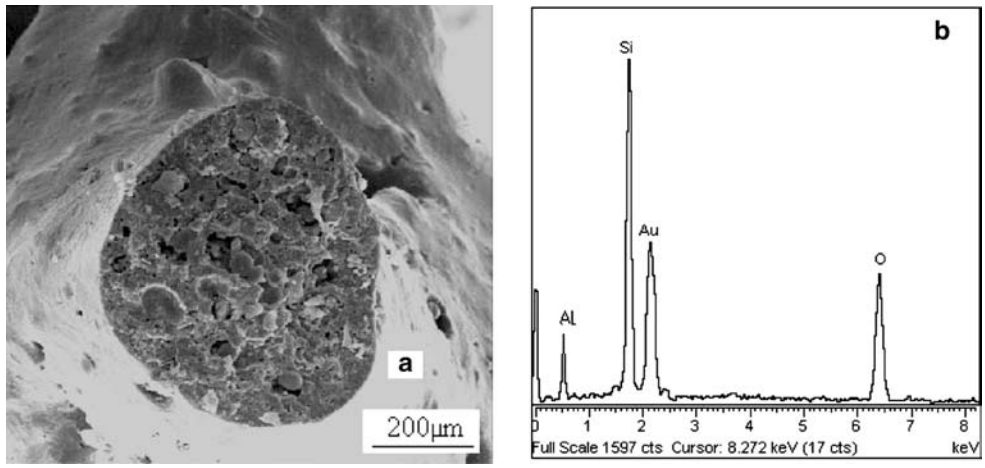

Fig. 6 SEM image of the cross-section microstructure of Si_3N_4 porous ceramic showing the oxide film (Al_2O_3 and SiO_2)

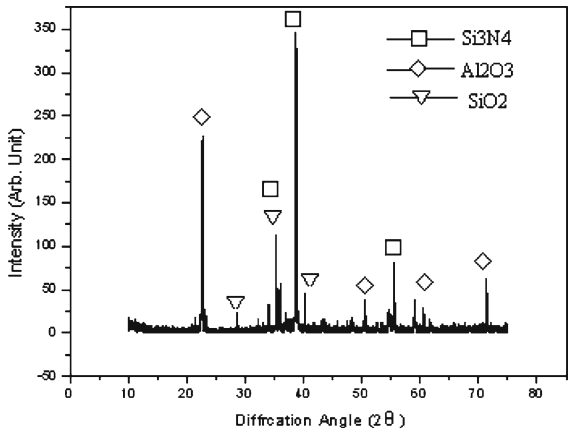

Fig. 7 XRD analyses of the strut surface of Si_3N_4 porous ceramic

thin spinel layer at the ceramic/metal interface plays a good and beneficial role in MMCs [14, 20]. Other authors give a inversed conclusion [21, 22]. The relations between compression stress and strain as magnesium alloy un-reinforced by ceramic form (specimen *A*) and two different composites reinforced by Si_3N_4 ceramic foam with different interface character (specimen *B* and *C*) are studied in this paper (which are shown in Fig. 9). Figure 10 shows the different interface microstructure of different composites. The interface of 3DNMMCs shown in Fig. 10a is worse and wider than that of 3DNMMCs shown in Fig. 10b. The width of interface in Fig. 10a is 6000 nm, whereas the width of interface in Fig. 10b is 500 nm. Comparatively, 3DNMMCs of Fig. 10b has more excellent interface structure characteristics. Interface structure characteristics such as interface width, interface crack and interface debonding are the main failure mechanism of composites. From Fig. 10a (bending arrow), the interface debonding and crack were observed distinctly whereas that in Fig. 10b is not only thin but also compact. So the composites providing with the interface in Fig. 10b were affirmed to be excellent than that of in Fig. 10a.

The values of the elastic modul E_A = 45 GPa, E_{RB} = 58 GPa, E_{RC} = 60 GPa, E_A as the elastic modul of magnesium alloy (specimen *A*), E_{RB} as the elastic modul of specimen *B* and E_{RC} as the elastic modul of specimen *C*. The values of rupture modul σ_{fA} = 240 MPa, σ_{fRB} = 250 MPa, σ_{fRC} = 255 MPa,σ_{fA} as the rupture modul of magnesium alloy, σ_{fRB} as the rupture modul of specimen *B* andσ_{fRC} as the rupture modul of specimen *C*. The un-reinforced magnesium alloys show a high elongation without necking of more than 25% at room temperature on the condition of enduring the compressive stress. The composites have a shorter elongation of 10% at room temperature. The composite (b) has a higher compression stress than composite (a) at the same strain although they have the same elongation. Other properties such as tensile and elongation with different interface are shown in Table 2.

Conclusions

One Si_3N_4/Mg composite reinforced by ceramic interpenetrating network structure has been fabricated via pressureless infiltration technology. The porous ceramic skeleton had a special microstructure with a hollow strut, which was padded by the sintering additives. Some interface reactions occurred on the ceramic/metal interface due to the strut surface of porous ceramic covered with a thin oxide film. The oxide film is proved as Al_2O_3 and SiO_2 by SEM, XRD and ESA. A thin $MgAl_2O_4$ spinel layer is observed in the present work. The special microstructure of ceramic–metal composites with an interpenetrating network, which creates their special properties, encourages to work on the synthesis of these materials and to investigate their microstructure and properties. Especially, the composites with a thin spinel layer located on the ceramic/metal interface possess excellent properties. It will give an opportunity to develop an interpenetrating network of ceramic–metal composites.

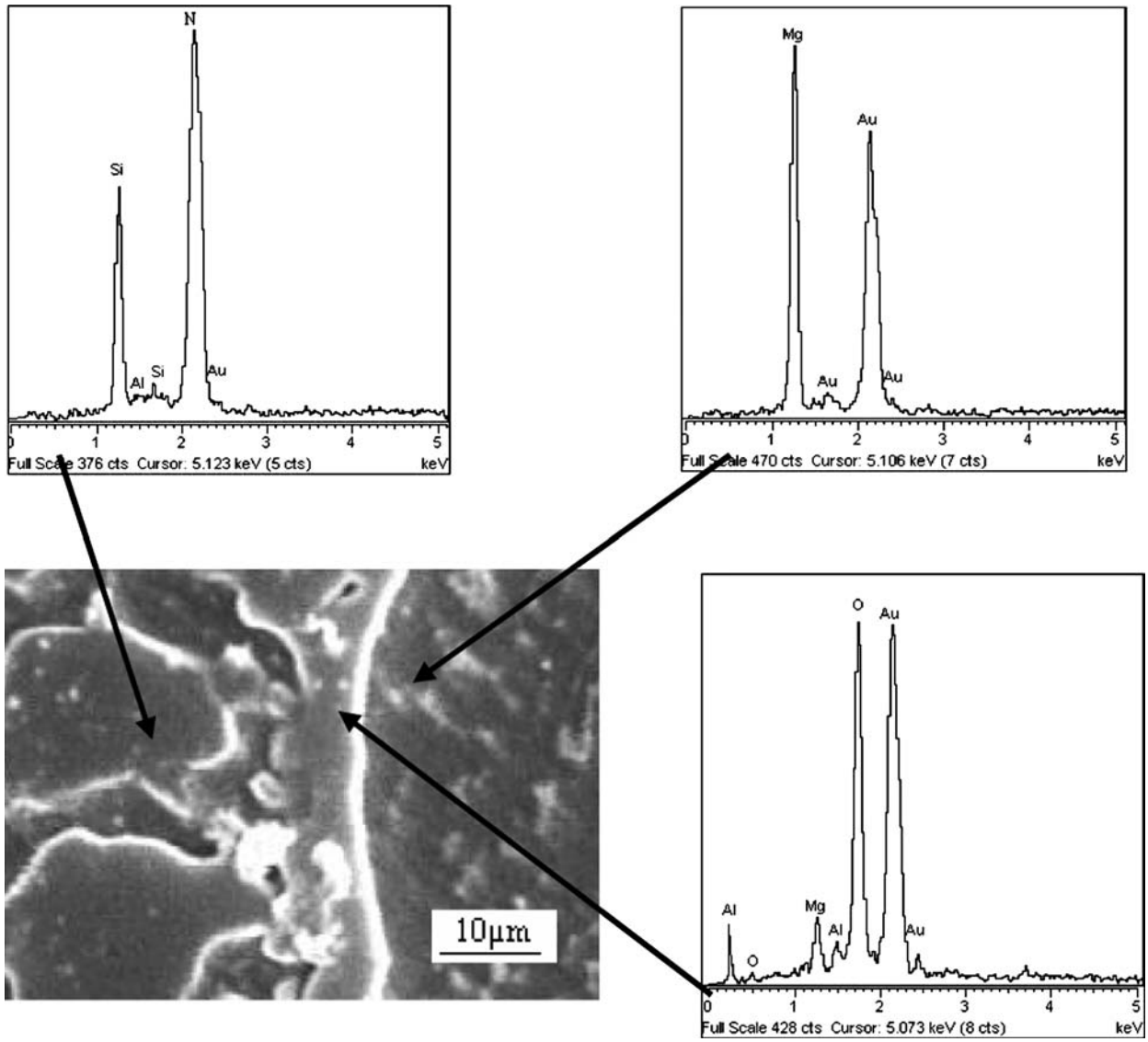

Fig. 8 SEM image of the microstructure of Si_3N_4/Mg composites showing the distribution of the $MgAl_2O_4$ spinel

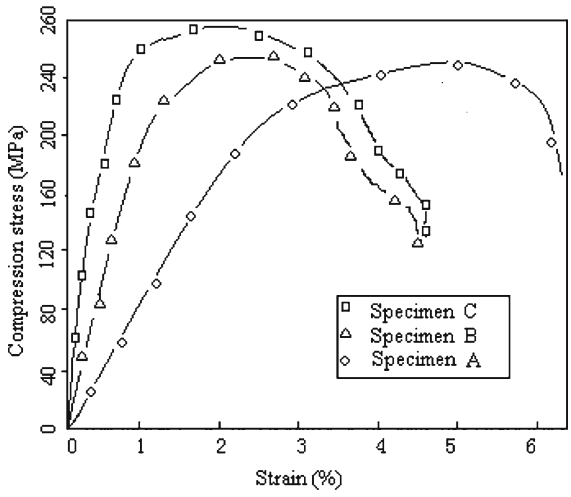

Fig. 9 The compression stress–strain relations of alloy and composites

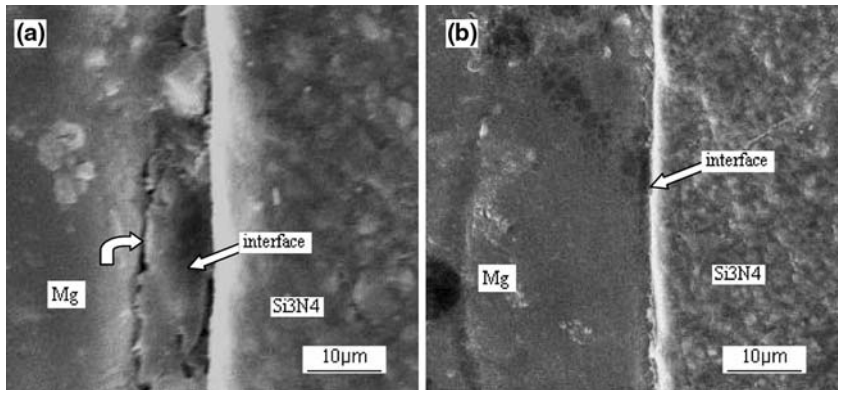

Fig. 10 The different interface microstructure of Si_3N_4/Mg composites

Acknowledgement This research was granted by Natural Science Foundation of China (50371047).

References

1. Wang HY, Jiang QC, Zhao YQ (2004) Mater Sci Eng A 372:109
2. Trojanova Z, Lukac P, Riehemann W, Mordike BL (2002) Mater Sci Eng A 324:122
3. Xu ZR, Chawla KK, Wolfenden A, Neuman A, Liggett GM, Chawla N (1995) Mater Sci Eng A 203:75
4. Konopka K, Olszowka-Myalska A, Szafran M (2003) Mater Chem Phys 81:329
5. Lu L, Lai MO, Froyen L (2002) Key Eng Mater 230(2):28
6. Ibrahim IA, Mohamed FA, Lavernia J (1991) J Mater Sci 26:1137
7. Breslin MC, Rignalda J, Xu L, Fuller M, Seeger J, Dahen GS, Otani T, Fraser HL (1995) Mater Sci Eng 195:113
8. Daehn GS, Starck B, Xu L, Elfishawy KH, Rignalda J, Fraser HL (1996) Acta Mater 44:249
9. Liu W, Koster U (1996) Scr Mater 35:35
10. Zeschky J, Goetz-Neunhoeffer F, Neubauer J, Jason Lo SH, Kummer B, Scheffler M, Greil P (2003) Composites Sci Technol 63:2361
11. Green DJ (1984) Fabrication and mechanical properties of lightweight ceramics produced by sintering of hollow spheres. Final report on AFOSR contract No.F49620-83-C0078
12. Schwartzwalder K, Somers AV (1963) Method of making porous ceramic articles. U.S. Patent 3090094
13. Green DJ (1983) J Am Ceram Soc 66:288
14. Konopka K, Olszówka-Myalska A, Szafran M (2003) Mater Chem Phys 81:329
15. Szafran M, Wisniewski P (2001) Colloid Surf. 179:201
16. De Hoff RT, Rhines FN (1968) Quantitative microscopy [M], McGraw-Hill, New York, 93
17. Gibson LJ, Ashby MF (1999) Cellular solids, structure and properties. 2nd edn. Cambridge University Press, Cambridge
18. Srinivasa Raw B, Jayaram V (2001) Acta Mater. 49:2373
19. Scholz H, Günther R, Rodel J, Greil P (1993) J Mater Sci Lett 12:939
20. Antonio Forn M, Baile T, Ruperez E (2003) J Mater Process Technol 143–144:58
21. Ding DY, Wang DZ, Zhang WL, Yao CK, Rao JC, Li DX (2000) Mater Lett 45:6
22. Vicens J, Chedru M, Chermant JL (2002) Composites: Part A 33:1421